RESEARCH ARTICLE SUMMARY

CELL BIOLOGY

Lysosomal cystine mobilization shapes the response of TORC1 and tissue growth to fasting

Patrick Jouandin*†, Zvonimir Marelja†, Yung-Hsin Shih, Andrey A. Parkhitko, Miriam Dambowsky, John M. Asara, Ivan Nemazanyy, Christian C. Dibble, Matias Simons*‡, Norbert Perrimon*‡

INTRODUCTION: Adaptation to changes in diet involves a complex cellular response controlled by interacting metabolic and signaling pathways. During fasting periods, this response remobilizes nutrients from internal stores through catabolic programs. In *Drosophila*, the fat body, an organ analogous to the liver and adipose tissue in mammals, functions as the organism's main energy reserve, integrating nutrient status with energy expenditure. How the fat body sustains its own needs and balances remobilization of nutrients over the course of a starvation period during developmental growth is unclear.

RATIONALE: The target of rapamycin complex 1 (TORC1) signaling pathway is a master regulator of growth and metabolism. Activated when nutrients are replete, TORC1 promotes biosynthesis and represses catabolic processes such as autophagy. In the fat body of fasting animals, however, TORC1 activity is dynamic. Activated to a maximum in feeding animals, TORC1 is acutely down-regulated at the onset of fasting, followed by partial and progressive reactivation through the amino acids generated by proteolysis during autophagy. This reactivation hints at a model in which TORC1 reaches a specific activity threshold allowing for minimal anabolism to occur concomitantly with catabolism, such as autophagy. To analyze how TORC1 dynamics is achieved, we used screening approaches, combined metabolomics with genetics, and developed specific heavy isotope–tracing methods in intact animals.

RESULTS: A screen to test the role of amino acids on animal fitness when starved on a low-protein diet identified cysteine as a potent suppressor of growth. During fasting, cysteine concentration was elevated through lysosomal cystine export through dCTNS, the mammalian ortholog of which, cystinosin, is responsible for the lysosomal storage disease cystinosis. dCTNS depletion and overexpression, respectively, lowered and elevated cysteine concentration in fasted animals, providing us with a genetic means with which to manipulate cysteine levels in vivo. Parallel metabolomics profiling of fasting animals revealed an increased concentration of tricarboxylic acid (TCA) cycle intermediates during fasting. Moreover, heavy isotope cysteine tracing demonstrated cysteine metabolism to coenzyme A (CoA) and further to acetyl-CoA, a process that was coupled to lipid catabolism in the fat body during fasting. Acetyl-CoA appeared to facilitate incorporation of additional substrates in the TCA cycle, with dCTNS overexpression increasing the entry of a heavy isotope alanine tracer in the TCA cycle. The elevation of TCA cycle intermediates by cysteine metabolism could be linked to the reactivation of TORC1. dCTNS overexpression dampened the reactivation of TORC1 during fasting, and it was sufficient to suppress TORC1 activity and cause ectopic autophagy in the fat body of fed animals. By contrast, dCTNS deletion did not affect TORC1 activity nor autophagy in fed animals but elevated the reactivation of TORC1 above a threshold suitable to halt autophagy during fasting. Finally, we show that cysteine metabolism regulates anaplerotic carbon flow in the TCA cycle and the level of amino acids, in particular aspartate. Combinatorial amino acid treatments rescued TORC1 activity upon fasting when cysteine levels were high. This suggests that the balance between cysteine metabolism and amino acid synthesis by the TCA cycle ultimately controls TORC1 reactivation, and thereby autophagy, during fasting. As a consequence, dCTNS depletion shortened life span during fasting, which could be restored by dietary cysteine, highlighting the central role of cysteine in the metabolism of fasted animals.

CONCLUSION: We found that in developing animals, adipose cells control biosynthesis during fasting by channeling nutrients between the lysosome and the mitochondria. After autophagy induction, amino acids are released from the lysosome, and some serve as substrates for the TCA cycle to replenish carbons in the mitochondria. Nutrients appear to be transiently stored in the form of TCA cycle intermediates and then extracted for the synthesis of amino acids that promote the reactivation of TORC1. We uncovered a new regulatory role for the metabolism of cysteine to acetyl-CoA during this process. By facilitating the incorporation of carbons into the TCA cycle and limiting amino acid synthesis, cysteine appears to regulate the partitioning of carbons in the TCA cycle. We propose that cysteine acts in a negative metabolic feedback loop that antagonizes TORC1 reactivation upon fasting above a threshold that would compromise metabolic homeostasis and animal fitness. ■

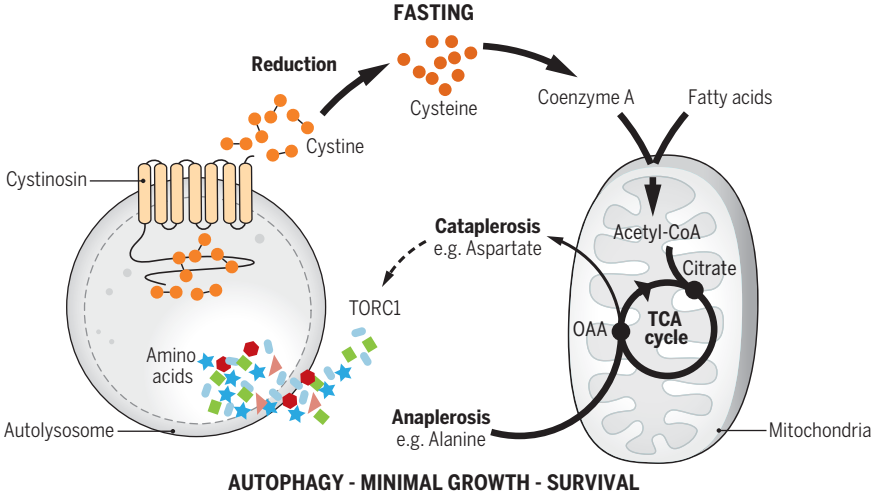

Cysteine metabolism acts in a negative feedback loop to maintain autophagy during fasting. The lysosomal transporter Cystinosin exports cystine, which is further reduced to cysteine in the cytosol. Cysteine is metabolized to coenzyme A (CoA) and fuels acetyl-CoA metabolism. Cysteine metabolism drives anaplerotic substrates into the TCA cycle and limits biosynthesis from oxaloacetate (OAA). This process is particularly important during fasting to regulate the reactivation of TORC1 and control autophagy.

The list of author affiliations is available in the full article online.
*Corresponding author. Email: Patrick_Jouandin@hms.harvard.edu (P.J.); matias.simons@med.uni-heidelberg.de (M.S.); perrimon@receptor.med.harvard.edu (N.P.)
†These authors contributed equally to this work.
‡These authors contributed equally to this work.
Cite this article as P. Jouandin *et al.*, *Science* **375**, eabc4203 (2022). DOI: 10.1126/science.abc4203

RESEARCH ARTICLE

CELL BIOLOGY

Lysosomal cystine mobilization shapes the response of TORC1 and tissue growth to fasting

Patrick Jouandin[1]*†, Zvonimir Marelja[2,3]†, Yung-Hsin Shih[3], Andrey A. Parkhitko[1], Miriam Dambowsky[2], John M. Asara[4,5], Ivan Nemazanyy[6], Christian C. Dibble[7,8], Matias Simons[2,3]*‡, Norbert Perrimon[1,9]*‡

Adaptation to nutrient scarcity involves an orchestrated response of metabolic and signaling pathways to maintain homeostasis. We find that in the fat body of fasting *Drosophila*, lysosomal export of cystine coordinates remobilization of internal nutrient stores with reactivation of the growth regulator target of rapamycin complex 1 (TORC1). Mechanistically, cystine was reduced to cysteine and metabolized to acetyl-coenzyme A (acetyl-CoA) by promoting CoA metabolism. In turn, acetyl-CoA retained carbons from alternative amino acids in the form of tricarboxylic acid cycle intermediates and restricted the availability of building blocks required for growth. This process limited TORC1 reactivation to maintain autophagy and allowed animals to cope with starvation periods. We propose that cysteine metabolism mediates a communication between lysosomes and mitochondria, highlighting how changes in diet divert the fate of an amino acid into a growth suppressive program.

Organisms cope with variations in diet by adjusting their metabolism. Specific organs integrate the availability of nutrients and respond to maintain systemic homeostasis. In fasting animals, the liver remobilizes nutrients through gluconeogenesis and β-oxidation of fatty acids to support peripheral tissue function (*1*, *2*). Variation in nutrient availability induces parallel changes in activity of signaling pathways, which resets intracellular metabolic turnover. The target of rapamycin complex 1 (TORC1) signaling pathway integrates sensing of amino acids and other nutrients with signals from hormones and growth factors to promote growth and anabolism (*3*). Nutrient scarcity inhibits TORC1 to limit growth and promote catabolic programs, including autophagy, which recycles internal nutrient stores to promote survival (*4*). Autophagy sequesters cytosolic material into autophagosomes that fuse with lysosomes for cargo degradation and recycling. The lysosomal surface is also the site where nutrient and growth factor–sensing pathways converge to activate TORC1. Degradation within autolysosomes generates new amino acids that in turn fuel metabolic pathways, including the tricarboxylic acid (TCA) cycle and gluconeogenesis, and reactivate TORC1, altogether maintaining minimal anabolism and growth (*5*–*8*). However, how organisms regulate the limited pools of remobilized nutrients and balance homeostatic metabolism with anabolic TORC1 activity over the course of starvation is poorly understood.

[1]Department of Genetics, Blavatnik Institute, Harvard Medical School, Boston, MA 02115, USA. [2]Université de Paris, INSERM, IHU *Imagine* – Institut des maladies génétiques, Laboratory of Epithelial Biology and Disease, 75015 Paris, France. [3]Institute of Human Genetics, University Hospital Heidelberg, 69120 Heidelberg, Germany. [4]Division of Signal Transduction, Beth Israel Deaconess Medical Center, Boston, MA 02115, USA. [5]Department of Medicine, Harvard Medical School, Boston, MA 02175, USA. [6]Platform for Metabolic Analyses, Structure Fédérative de Recherche Necker, INSERM US24/CNRS UMS 3633, Paris 75015, France. [7]Department of Pathology and Cancer Center, Beth Israel Deaconess Medical Center, Boston, MA 02115, USA. [8]Department of Pathology, Harvard Medical School, Boston, MA 02115, USA. [9]Howard Hughes Medical Institute, Harvard Medical School, Boston, MA 02115, USA.
***Corresponding author. Email: Patrick_Jouandin@hms.harvard.edu (P.J.); matias.simons@med.uni-heidelberg.de (M.S.); perrimon@receptor.med.harvard.edu (N.P.)**
†These authors contributed equally to this work.
‡These authors contributed equally to this work.

Results

TORC1 signaling is reactivated in vivo during prolonged fasting

To study the regulation of metabolism and TORC1 signaling in vivo, we used the *Drosophila* larval fat body, an organ analogous to the liver and adipose tissue in mammals. The fat body responds to variations in nutrient availability through TORC1 signaling, which in turn regulates systemic larval growth rate by the secretion of growth factors from distant organs (*9*, *10*). When larvae were fasted, i.e., completely deprived of their food source but kept otherwise hydrated, TORC1 signaling in the fat body was acutely decreased at the onset of fasting. However, prolonged fasting led to partial and progressive reactivation of TORC1 over time, as measured by phosphorylation of the specific TORC1 substrate S6K (Fig. 1A). This process was dependent on autophagy induction (fig. S1, A and B), consistent with autophagy facilitating amino acid recycling and TORC1 reactivation in mammalian cells (*6*, *8*). To understand how changes in nutrients and metabolites intersect with TORC1 signaling during this fasting response, we used two complementary, unbiased approaches: (i) a targeted mass spectrometry–based screen for polar metabolites altered during fasting and (ii) a larval growth screen to test the effects of individual amino acids in animals fed a low-protein diet.

Interplay between TORC1 signaling and the TCA cycle during fasting

In the first screen, metabolic profiling of whole animals revealed depletion of most metabolites over the course of fasting (Fig. 1B). By contrast, multiple TCA cycle intermediates accumulated over time, in particular citrate and isocitrate. This appeared not to result from defective TCA cycle activity upon fasting because U-$^{13}C_6$-glucose oxidation in the TCA cycle was functional and the ratios between NADH and NAD^+ were comparable between fed and fasting conditions (fig. S2, A and B). Similar metabolomic profiles were observed in fat bodies from fed and fasted animals (Fig. 1B), indicating that TORC1 reactivation in the fat body correlates with accumulation of TCA cycle intermediates, in particular citrate and isocitrate. Next, we tested whether TORC1 activity affects the accumulation of TCA cycle intermediates during fasting. For this, we measured the concentrations of TCA cycle intermediates in fed and fasted larvae of GATOR1 (*nrpl2*$^{-/-}$) and GATOR2 (*mio*$^{-/-}$) mutants, which exhibit constitutive activation or suppression of TORC1 signaling, respectively (*11*, *12*) (fig. S3A). Activation of TORC1 in GATOR1 mutants blunted the elevation of the concentration of TCA cycle intermediates normally observed during fasting. Conversely, inhibition of TORC1 in GATOR2 mutants raised the concentration of TCA cycle intermediates in fed animals, suggesting that the accumulation of TCA cycle intermediates during fasting requires TORC1 inhibition. We also tested whether changes in the TCA cycle during fasting affects TORC1 reactivation by targeting pyruvate carboxylase (PC). PC serves an anaplerotic function by replenishing oxaloacetate (OAA) and hence other TCA cycle intermediates (Fig. 1C), a process that regulates gluconeogenesis and regeneration of amino acids (*1*). Depletion of PC (*pcb/CG1516*) in the larval fat body increased the concentration of the PC substrate alanine in the fat body (fig. S3B) (*1*). Consistent with impaired TCA cycle activity, depletion of PC elevated the level of OAA and the ratio between NAD(P) and NAD(P)H while decreasing the levels of other TCA cycle intermediates as well as cataplerotic products such as asparagine, intermediates of the urea cycle, carbamoyl aspartate, and inosine 5′-monophosphate (IMP)

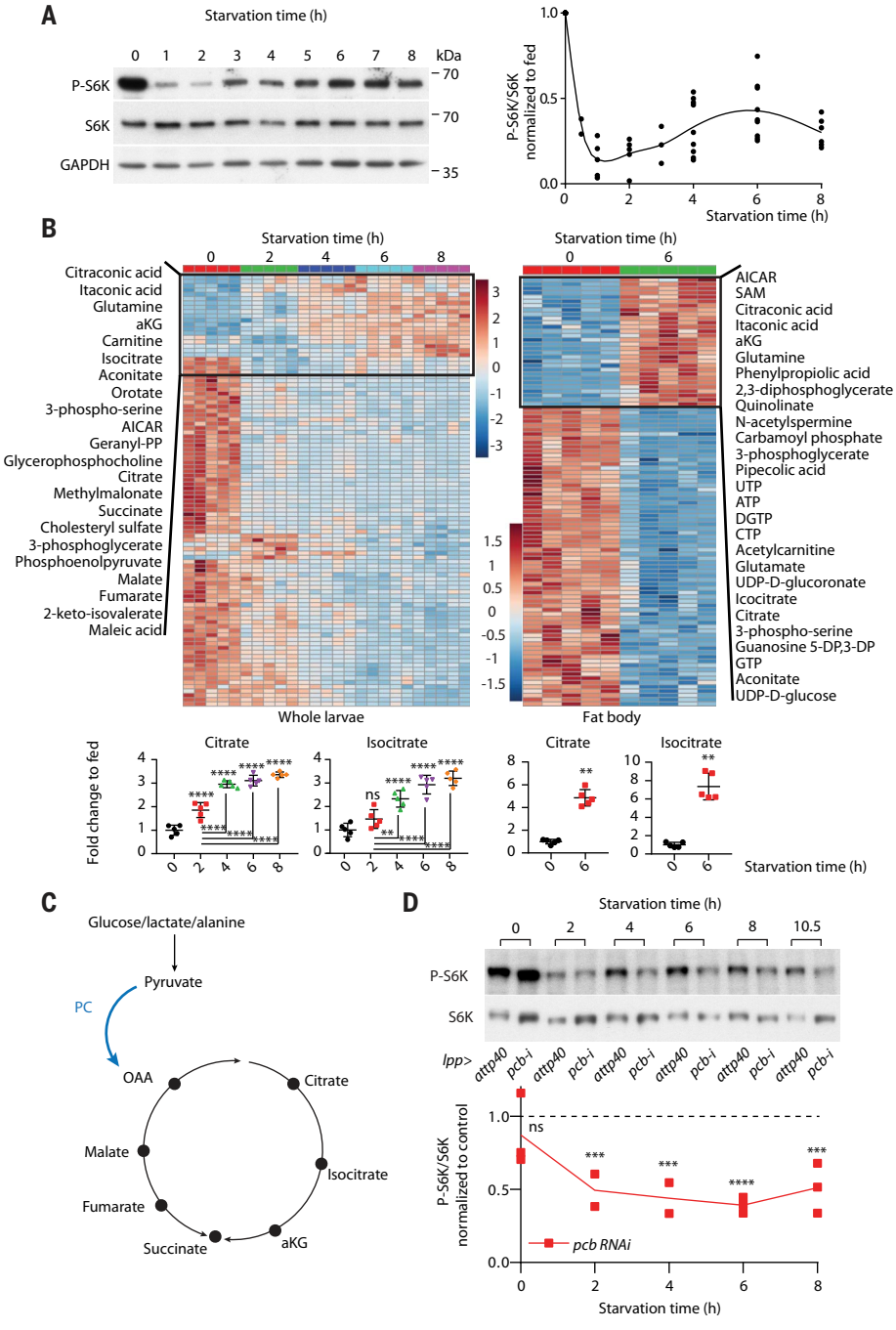

Fig. 1. TORC1 reactivation upon prolonged fasting correlates with increase of TCA cycle intermediates. (**A**) Prolonged fasting leads to TORC1 reactivation. Phosphorylation levels of the direct TORC1 target S6K in dissected fat bodies from fasting larvae (i.e., placed on a tissue soaked in PBS). (**B**) Heatmap metabolite levels (LC-MS/MS) from whole mid-third-instar larvae (left) or dissected fat bodies (right), fed (0h) and fasted. Lower panels are individual plots from the same dataset. (**C**) Schematic of anaplerosis through PC. (**D**) Knockdown of *pcb*/PC suppresses mTORC1 reactivation upon prolonged fasting. For (B) and (D), data are shown as mean ± SD. ns, $P \geq 0.05$; $^{**}P \leq 0.01$; $^{***}P \leq 0.005$; $^{****}P \leq 0.0001$ (see the materials and methods for details).

(fig. S3B). Depletion of PC also suppressed TORC1 reactivation during fasting (Fig. 1D), supporting the functional link between the TCA cycle and TORC1 signaling. These data suggest that at the onset of fasting, TORC1 inhibition appears necessary to raise the concentration of TCA cycle intermediates, which in turn affect TORC1 reactivation, possibly through the synthesis of building blocks downstream of PC, i.e., cataplerosis.

Cysteine suppresses growth in a TORC1-dependent manner

In the second screen, we tested the effects of supplementation with single amino acids on growth of larvae fed a low-protein diet (see the supplementary materials) (Fig. 2A). Fasting and a low-protein diet may trigger distinct metabolic states with intrinsic differences, but both protocols trigger a starvation response. Supplementation of food with cysteine suppressed growth in larvae to a distinctly greater extent than any other amino acid, and this phenotype was accentuated in a low-protein diet (see the supplementary text S1 and fig. S4, A to D). The inhibition of growth by cysteine was interdependent with TORC1 signaling, because cysteine treatment partially inhibited TORC1 activity in fat bodies and constitutive activation of TORC1 in GATOR1-null (*nprl2*$^{-/-}$) mutants (*12*) and partially restored growth under cysteine supplementation (fig. S5, A to E). Conversely, cysteine supplementation did not further suppress growth in mutants with constitutive suppression of TORC1 activity caused by either loss of GATOR2 (*mio*$^{-/-}$) or overexpression of TSC complex subunits (*lpp>UAS-TSC1, UAS-TSC2*) in the fat body (fig. S5, E and F). Altogether, these data suggest that cysteine has a specific inhibitory effect on growth and TORC1 signaling in larvae fed a low-protein diet, and that this growth suppression requires suppression of TORC1 signaling.

Lysosomal cystine transporter dCTNS regulates cysteine level during fasting

The results of our two screens led us to explore the relationship among cysteine metabolism, the TCA cycle, and TORC1 during fasting. Cysteine concentrations increased during fasting (Fig. 2B and fig. S6A) (*13*), and cysteine treatment increased the concentration of TCA cycle intermediates, particularly for animals fed a low-protein diet (fig. S6B). To further understand this effect of cysteine, we searched for its intracellular source during fasting. Abolishing autophagy in the fat body decreased cysteine levels upon fasting (fig. S7A), suggesting that autolysosomal function regulates cysteine balance. Thus, we focused on the role of the lysosomal cystine transporter cystinosin in recycling cysteine during fasting. Cystinosin, which is encoded by *CTNS* in mammals, is mutated in the lysosomal storage disorder cystinosis and has been implicated in the regulation of TORC1 signaling and autophagy (*14*–*16*). Endogenous tagging of the *Drosophila* ortholog *CG17119* (hereafter referred to as *dCTNS*) confirmed its specific lysosomal localization in cells of the fat body (fig. S7, B and C). *dCTNS*$^{-/-}$ larvae showed accumulation of cystine (fig. S7D), consistent with a role for cystinosin in lysosomal cystine transport (Fig. 2C). In fed conditions, control and *dCTNS*$^{-/-}$

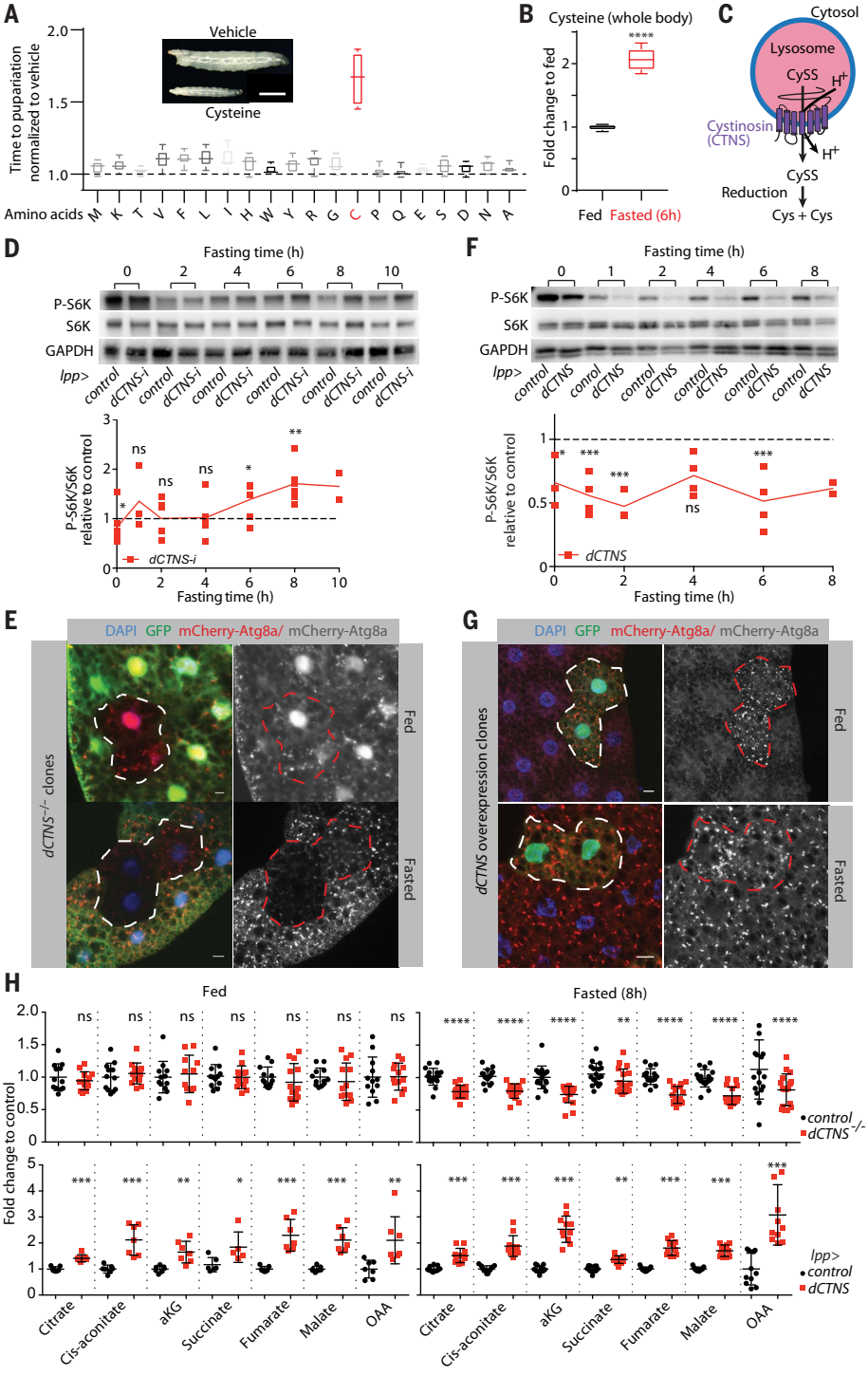

Fig. 2. Lysosome-derived cysteine promotes elevation of TCA cycle intermediates and antagonizes TORC1 reactivation. (**A**) Amino acid screen reveals cysteine as a growth suppressor. Time to pupariation for larvae fed a low-protein diet supplemented with the indicated amino acids all along development (see supplementary materials and methods for concentrations; the cysteine concentration is 5 mM). Scale bar, 1 mm. (**B**) Cysteine levels in whole control larvae (*lpp>attp40*) ($N = 5$). (**C**) Schematic of lysosomal cystine (CySS) efflux through cystinosin/*CTNS*. (**D**) Loss of *Drosophila* cystinosin in the fat body (*lpp>dCTNS RNAi, dCTNS-i*) leads to higher TORC1 reactivation upon prolonged fasting. *P*-S6K levels in dissected fat bodies from larvae fasted for the indicated time. *lpp>white RNAi*, control background. (**E**) dCTNS maintains autophagy during fasting. *dCTNS*$^{-/-}$ clones (non-GFP, outlined) in 80-hour AEL larvae expressing mCherry-Atg8a fasted for 8 hours. Scale bar, 10 μm. (**F**) *dCTNS* overexpression suppresses TORC1 activity. *P*-S6K levels in dissected fat bodies from larvae fasted for the indicated time. *Lpp>GFP RNAi (GFP-i)*, control background. (**G**) *dCTNS* overexpression induces autophagy. *dCTNS* overexpression clones (GFP marked, outlined) in 80-hour AEL larvae. Scale bar, 10 μm. (**H**) dCTNS regulates TCA cycle intermediate levels upon fasting. Relative metabolites levels measured by LC-MS/MS in 80-hour AEL larvae fed or fasted for 8 hours. Controls are dCTNS$^{+/-}$ (upper graphs) or GFP-i (lower graphs). For (B), (D), (F), and (H), data are shown as mean ± SD. ns, $P \geq 0.05$; *$P \leq 0.05$; **$P \leq 0.01$; ***$P \leq 0.005$; ****$P \leq 0.0001$ (see the materials and methods for details).

larvae showed similar abundance of cysteine, likely reflecting dietary intake as the main source of cysteine. By contrast, in fasting animals, cysteine concentration dropped in *dCTNS*$^{-/-}$ larvae (fig. S7E). Conversely, *dCTNS* overexpression increased cysteine levels, which caused a developmental delay similar to cysteine treatment (fig. S7, F and G). In sum, our results indicate that dCTNS recycles cysteine from the lysosome during fasting.

Cytosolic cysteine synthesis compensates for defective lysosomal cystine export

To evaluate the contribution of cytosolic cysteine synthesis during fasting, we also analyzed the trans-sulfuration pathway, a process that requires cystathionine β-synthase (Cbs) (fig. S8A) (*17*, *18*). Depletion of *cbs* in the fat body reduced cysteine levels upon fasting, but this was not the case in fed animals. Cbs and dCTNS showed additive roles in maintaining cysteine concentration in fasted animals (fig. S8B), suggesting that the phenotypic effects of *dCTNS* deficiency are partially masked by the trans-sulfuration pathway. Because the trans-sulfuration pathway involves the breakdown of methionine, we found that *dCTNS* overexpression increased the concentration of the intermediates of the trans-sulfuration pathway, particularly methionine (fig. S8C). By contrast, methionine was depleted in

fasted *dCTNS* mutant animals (fig. S8C), suggesting that cysteine from lysosomal origin limits the activity of the trans-sulfuration pathway. Methionine is an essential amino acid, and dCTNS appears to limit its depletion upon fasting, a process possibly reminiscent of the methionine-sparing effect of dietary cystine previously observed in humans (*19*, *20*).

dCTNS affects TORC1 reactivation and the TCA cycle during fasting

Next, we analyzed the effect of cysteine recycling by dCTNS on TORC1 reactivation and the TCA cycle. Although *dCTNS* depletion in the larval fat body did not affect TORC1 inhibition at the onset of fasting, it slightly increased TORC1 reactivation upon prolonged fasting, as indicated by increased S6K phosphorylation (Fig. 2D) and cytosolic accumulation of Mitf/TFEB (fig. S9A). Analysis of *dCTNS*$^{-/-}$ fat body clones showed that increased TORC1 signaling was cell autonomous and sufficient to compromise maintenance of autophagy during fasting (Fig. 2E and fig. S9B). Accordingly, treatment with the TORC1 inhibitor rapamycin restored autophagy in *dCTNS*-deficient cells (fig. S9C). Conversely, *dCTNS* overexpression caused down-regulation of TORC1 in fed and fasting animals and induced ectopic autophagy in fed animals (Fig. 2, F and G). Metabolic profiling of *dCTNS*$^{-/-}$ animals showed a depletion of TCA cycle intermediates specifically during fasting, whereas they accumulated after overexpression of *dCTNS* in fed and fasted animals (Fig. 2H).

dCTNS is required for animal fitness during starvation

We also examined the role of *dCTNS* on starvation resistance. In normally fed animals, *dCTNS* deficiency delayed larval development but appeared to have no effect on the life span of adult flies (Fig. 3, A and B). However, *dCTNS*-deficient animals had an increased developmental delay when raised in a low-protein diet, and adults died more quickly from starvation (Fig. 3, B and C). Depletion of *dCTNS* specifically in the fat body did not affect development in fed animals but caused a developmental delay on a low-protein diet, consistent with the importance of dCTNS function in the fat body during fasting (Fig. 3B). The starvation sensitivity of *dCTNS*-deficient animals was decreased by low concentrations of rapamycin (that did not elevate cysteine concentration), indicating a possible role for altered TORC1 signaling and autophagy in mediating *dCTNS* growth phenotypes (Fig. 3D, fig. S9D; see supplementary text S2). The role of *dCTNS* during starvation was dependent on its cystine transport function as treatment with either cysteamine [which facilitates cystine export out of the lysosome independently of cystinosin (*21*)]

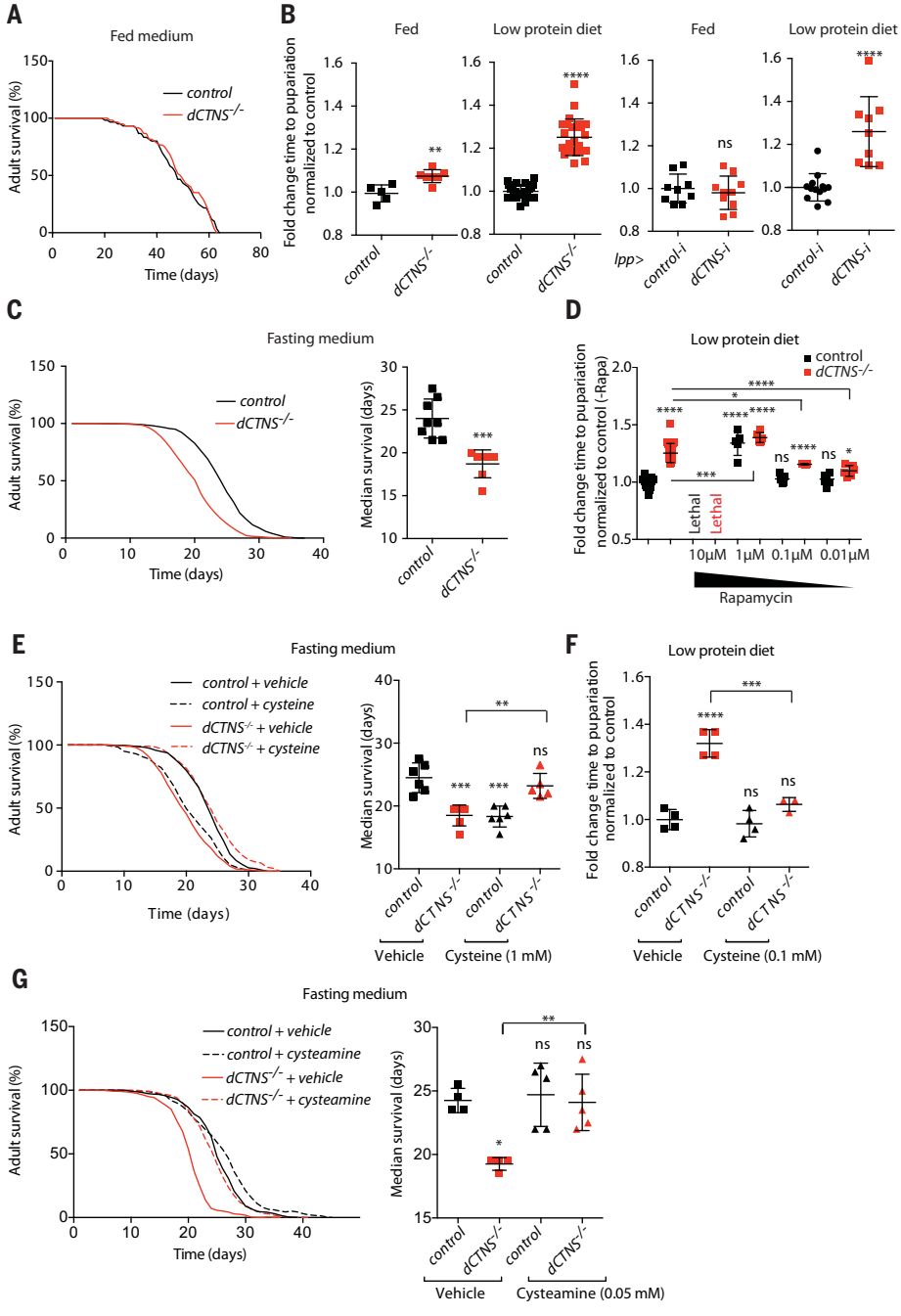

Fig. 3. *dCTNS* controls resistance to starvation through cysteine efflux and TORC1. (**A**) dCTNS does not affect life span in the fed condition. Life span of control (w^{1118}) and *dCTNS*$^{-/-}$ animals fed a standard diet (N = 2). (**B**) dCTNS in the fat body controls starvation resistance during development. Shown is the fold change time to pupariation for larvae of indicated genotype grown on control (fed) or low-protein diet. Controls are dCTNS$^{+/-}$ (left panel) or white RNAi (control-i, right panel). (**C**) dCTNS controls starvation resistance of adult animals. Survival of control (w^{1118}) and *dCTNS*$^{-/-}$ animals fed a chemically defined starved diet composed only of physiologically relevant ions, including biometals (see the materials and methods). (**D** to **F**) Low dose of rapamycin and cysteine treatments rescues starvation sensitivity of *dCTNS*$^{-/-}$ animals. Shown is the developmental time of larvae raised on a low-protein diet supplemented with the indicated concentration of rapamycin (D) or 0.1 mM cysteine (F) and survival of adult flies on chemically defined starved diet with or without 1 mM cysteine (E). Controls are *dCTNS*$^{+/-}$ [(D) and (F)] and w^{1118} (E). (**G**) Cysteamine treatment restores starvation resistance of *dCTNS*$^{-/-}$ animals. Shown is the life span of control (w^{1118}) and *dCTNS*$^{-/-}$ animals fed a chemically defined starved diet supplemented with 0.5 mM cysteamine or vehicle. For (B) to (G), data are shown as mean ± SEM. ns, $P \geq 0.05$; *$P \leq 0.05$; **$P \leq 0.01$; ***$P \leq 0.005$; ****$P \leq 0.0001$ (see the materials and methods for statistics details).

or low concentrations of cysteine (which did not affect development of control animals) decreased the starvation sensitivity of *dCTNS*$^{-/-}$ animals (Fig. 3, E to G). Altogether, we demonstrate the physiological importance of cysteine recycling from the lysosome through dCTNS during fasting, which supports the accumulation of TCA cycle intermediates and antagonizes TORC1 reactivation to maintain autophagy.

dCTNS connects with the TCA cycle through acetyl-CoA metabolism

To search for a mechanistic link between cysteine metabolism and the TCA cycle, we performed heavy isotope-labeled cysteine tracing experiments by feeding larvae either U-^{13}C-cysteine or $^{13}C_3$ $^{15}N_1$-cysteine. Consistent with cysteine metabolism in mammals, this revealed three major metabolic fates for cysteine: glutathione (GSH), taurine, and coenzyme A (CoA) (Fig. 4, A and B). CoA derived from labeled cysteine was subsequently used to form acetyl-CoA in the fat body of larvae fed a control and low-protein diet (Fig. 4, A and B, and fig. S10, A and B). We found that the starvation sensitivity of *dCTNS*$^{-/-}$ animals was partially suppressed by dietary treatment with pantethine, a disulfide intermediate of the CoA biosynthetic pathway downstream of cysteine incorporation (fig. S11, A and C), but not with pantothenic acid, the vitamin precursor upstream of cysteine incorporation during CoA synthesis (fig. S11B). This suggests that deficiencies in CoA synthesis caused by limiting cysteine availability contribute to the *dCTNS* phenotypes. To analyze how this affects the TCA cycle, we further focused on the direct flow of carbons from cysteine into acetyl-CoA. Upon feeding, the pyruvate dehydrogenase complex (PDHc) harvests the acetyl moiety from pyruvate and transfers it to CoA to generate acetyl-CoA (*22*) (fig. S12A). Upon fasting, PDHc activity decreases, draining pyruvate toward PC to support biosynthesis, whereas β-oxidation of fatty acids may provide the acetyl moiety for acetyl-CoA synthesis (*23*) (Fig. 5A and fig. S12A). In fed larvae overexpressing *dCTNS* in the fat body, depletion of the PDHc activator pyruvate dehydrogenase phosphatase (*pdp*) (*24*) normalized growth, TORC1 activity, and the concentration of TCA cycle intermediates (fig. S12, B to D). By contrast, when *dCTNS*-overexpressing larvae were fed a low-protein diet or fasted, PDHc inhibition failed to restore development or fully restore TORC1 activity, respectively, presumably reflecting the use of substrates other than pyruvate for acetyl-CoA synthesis under these conditions, such as acetate and fatty acids (fig. S12, B and C). In turn, depletion of CPT1/*whd*, the acylcarnitine transferase required for β-oxidation of fatty acids, restored growth of dCTNS-overexpressing larvae to a larger extent on a fed diet than on a low-protein diet, suggesting that increased cysteine metabolism is sufficient to promote β-oxidation upon feeding (fig. S12F). Accordingly, *dCTNS* overexpression increased the abundance of acetyl-CoA and decreased the abundance of acyl-carnitines and fatty acids in both fed and fasted animals. By contrast, in *dCTNS*$^{-/-}$ animals, acetyl-CoA levels were decreased, whereas acylcarnitines and fatty acids showed higher levels, specifically during fasting, which could be normalized by cysteamine treatment (Fig. 5,

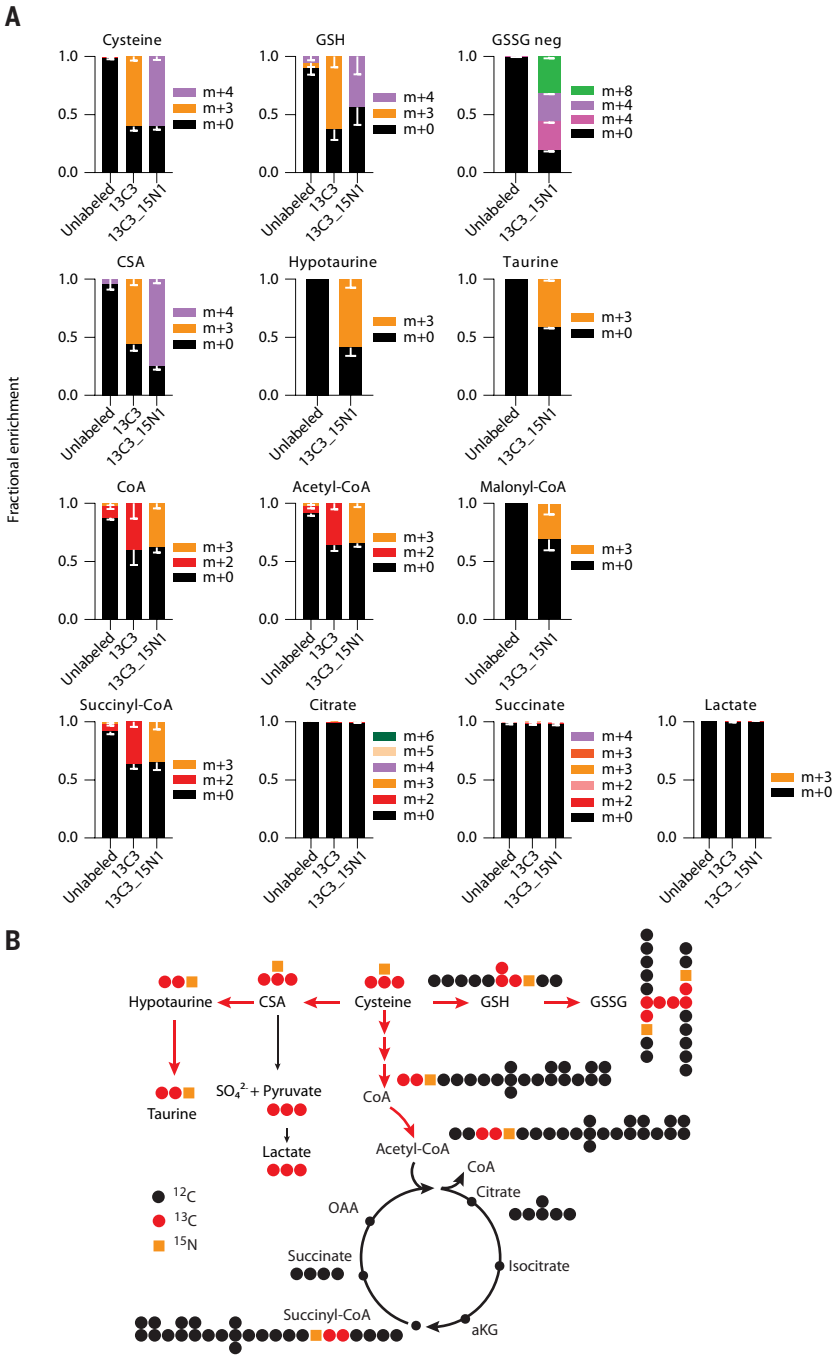

Fig. 4. Cysteine fuels de novo CoA/acetyl-CoA metabolism. (**A**) Mean fractional enrichment ± SD of U-^{13}C-cysteine (N = 10), $^{13}C_3$-$^{15}N_1$-cysteine (N = 5), or unlabeled samples (N = 10) in indicated metabolites measured by LC-MS/MS in whole larvae fast overnight with 5 mM tracer. m+n refers to the number of ^{13}C atoms (+n) added to the expected mass spectra of each measured isotopomer (m); m+0 means unlabeled. (**B**) Schematic of cysteine metabolism and labeling patterns from U-^{13}C-cysteine and $^{13}C_3$-$^{15}N_1$-cysteine tracers. Red arrows indicate main cysteine flux.

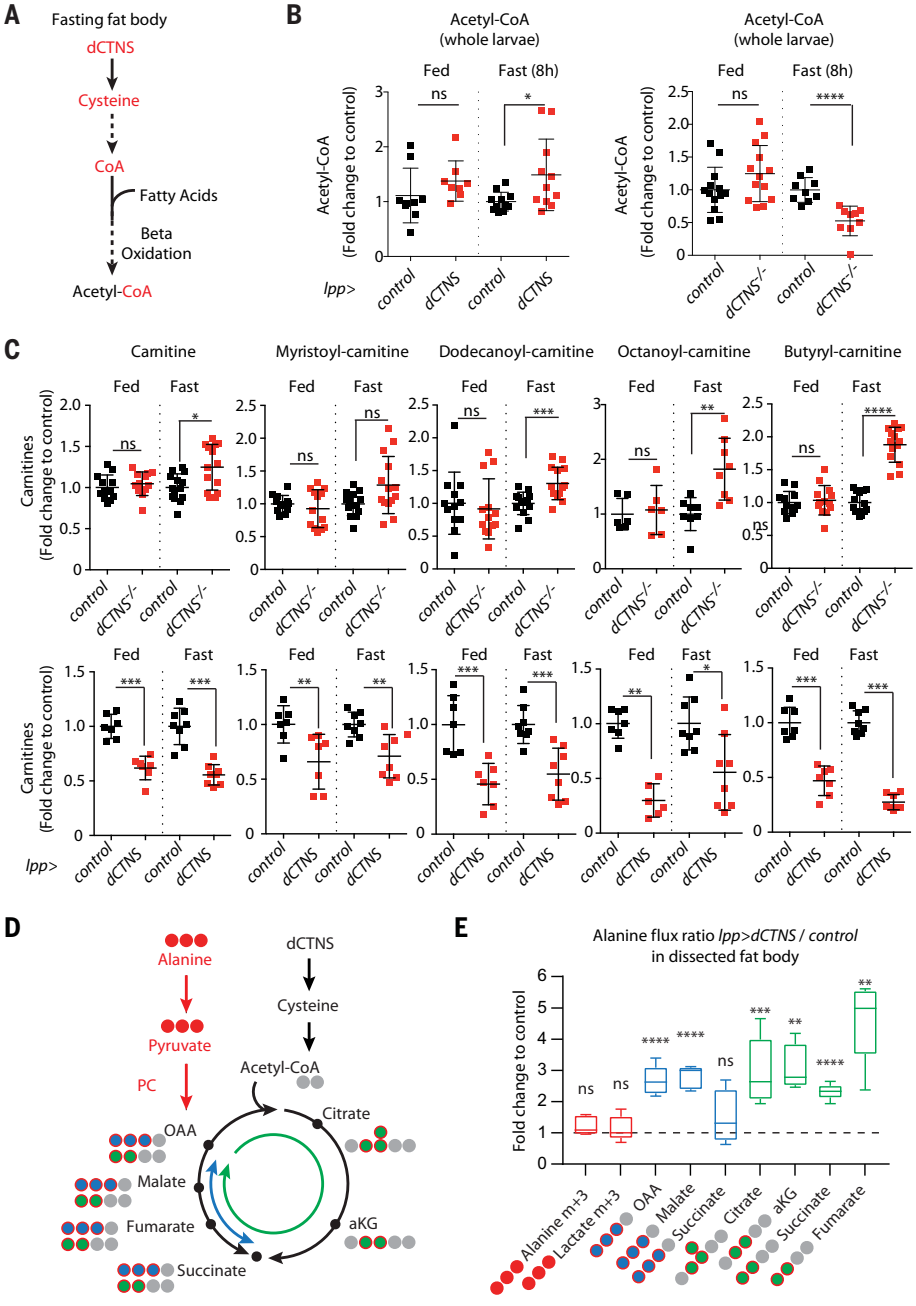

Fig. 5. Cysteine metabolism to acetyl-CoA affects the concentration of fatty acids and increases carbon flux through PC and the TCA cycle. (**A**) Schematic of acetyl-CoA synthesis during fasting. (**B** and **C**) Metabolite levels in whole third-instar larvae showing *dCTNS*$^{-/-}$ and *dCTNS* overexpression in the fat body. (**D**) Schematic of alanine carbon flux into the TCA cycle upon fasting. (**E**) Alanine flux ratio. Shown is the fold change *lpp>dCTNS*/control (*lpp>attp40*) for the indicated TCA cycle intermediates isotopomers measure by LC-MS/MS in dissected fat bodies from third-instar larvae fed a low-protein diet with 25 mM U-^{13}C-alanine for 6 hours.

B and C, and fig. S13, A and B). In addition, *dCTNS* overexpression was sufficient to deplete triglyceride stores in fed animals, whereas they slightly accumulated after depletion of *dCTNS* in the fat body upon fasting (fig. S13C). Altogether, our data suggest that during fasting, lysosomal cysteine mobilization is potentially rate limiting for de novo CoA synthesis, which in turn may promote acetyl-CoA production through β-oxidation of fatty acids remobilized from triglyceride stores. The precise contribution of acetyl moieties by fatty acids and other substrates for the synthesis of acetyl-CoA during fasting remains to be determined.

Lysosomal-derived cysteine may control TORC1 indirectly through the flow of amino acids in and out of the TCA cycle

Increased CoA synthesis from cysteine might enlarge the TCA cycle carbon pool in at least two ways: first, by providing the CoA required to accept increasing amounts of carbon from fatty acids to form acetyl-CoA, and second, by promoting anaplerosis of alternative carbon sources through the allosteric activation of PC by acetyl-CoA (*25*). To test whether increased production of acetyl-CoA supported by lysosomal cysteine efflux could increase anaplerosis, we analyzed alanine anaplerosis in the TCA cycle in animals overexpressing *dCTNS* in the fat body. We supplemented a low-protein diet with a [U-^{13}C]alanine tracer and followed the anaplerotic flux of alanine in the TCA cycle in dissected fat bodies (Fig. 5D). We used a tracer amount that had a negligible contribution to the total alanine pool and also did not affect cysteine metabolism to acetyl-CoA (fig. S14, A and B). *dCTNS* overexpression increased (by more than twofold) alanine anaplerosis as well as oxidative flux in the TCA cycle through citrate synthase (that consumes OAA and acetyl-CoA to generate citrate; Fig. 5E). We therefore propose that during fasting, cysteine recycling and metabolism to acetyl-CoA in the fat body supports anaplerosis through PC and flux through citrate synthase, thereby contributing to the accumulation of TCA cycle intermediates, in particular citrate and isocitrate.

During fasting, given the fixed and preestablished level of carbons available, increased abundance of TCA cycle intermediates may indicate the retention of anaplerotic inputs in the TCA cycle at the expense of their extraction for biosynthesis (i.e., cataplerosis). Because cataplerosis promotes amino acid synthesis (*1*), which in turn affects TORC1 signaling (*6*), we analyzed the effect of lysosomal cysteine recycling on individual amino acid pools. *dCTNS* overexpression in the fat body led to depletion of aspartate and downstream nucleotide precursors (IMP and uridine 5′-monophosphate), as well as, to a lesser extent, asparagine and glutamate (Fig. 6A and fig. S15, A and B). The abundances of aspartate and IMP were increased in fasted *dCTNS*$^{-/-}$ animals, and cysteamine treatment partially normalized their concentration (fig. S15C). Aspartate is a cataplerotic product of OAA (*1*), a process that involves glutamate oxaloacetate transaminase 2 (Got2). Cysteine metabolism may transiently trap anaplerotic carbons into the TCA cycle in fasted animals, away from their immediate extraction for biosynthesis. We analyzed whether cysteine metabolism could regulate growth and antagonize TORC1 reactivation through limiting the availability of glutamate and aspartate, because these amino acids are critical regulators of cell growth and have

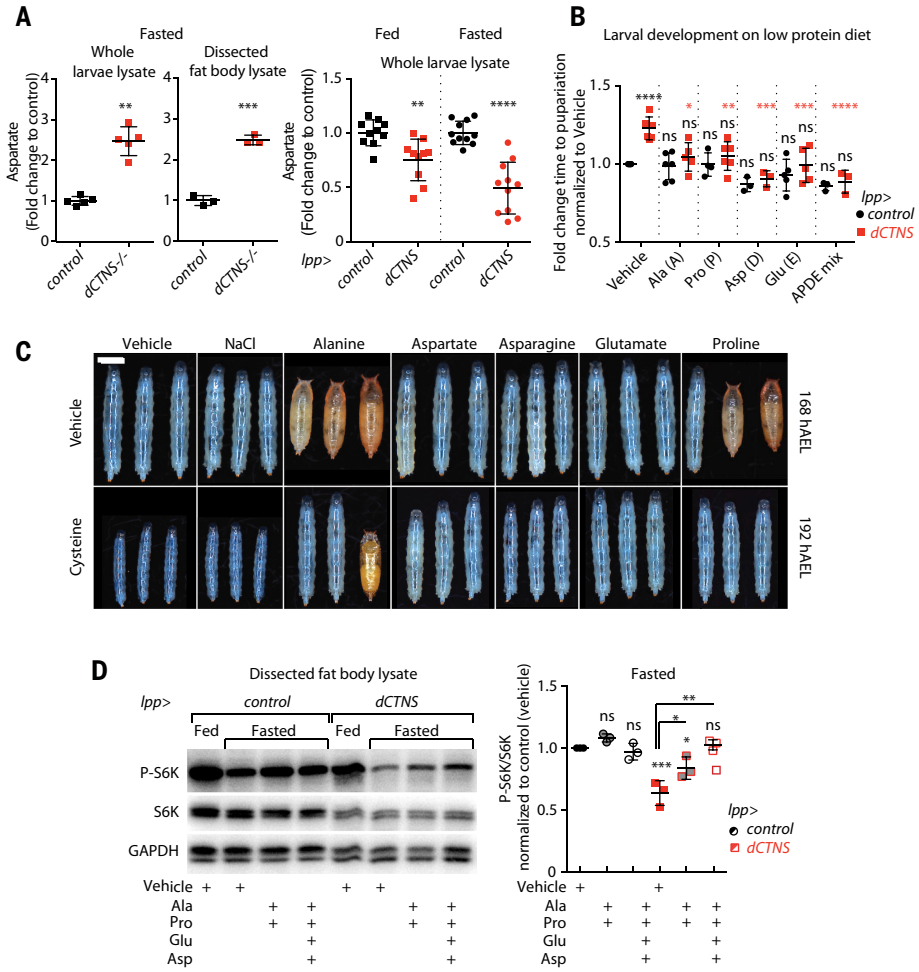

Fig. 6. Cysteine metabolism regulates TORC1 and growth through cataplerotic amino acids levels. (**A**) Relative levels of aspartate in 85-hour AEL larvae *dCTNS*$^{-/-}$ (whole larvae and fat body) and after dCTNS overexpression in the fat body. (**B**) Amino acid supplementation suppresses the developmental delay induced by *dCTNS* overexpression in the larval fat body. Shown is the fold change time to pupariation for larvae fed a low-protein diet with or without supplementation with the indicated amino acids (Ala, Pro, and Glu: 5 mM; Asp: 10 mM). Red asterisks show significance between dCTNS animals treated with vehicle versus amino acids. (**C**) Photographs of aged matched animals fed a low-protein diet with or without 5 mM cysteine with or without the indicated metabolites (25 mM each). Scale bar, 1 mm. (**D**) dCTNS-induced TORC1 inhibition is reversed by supplementation with the indicated amino acids. *P*-S6K levels in fat body from fed and fasted (6 hour) larvae of indicated genotypes. The 70- to 72-h AEL larvae were transferred to a low-protein diet with or without supplementation with the indicated amino acids (Ala and Pro: 20 mM; Asp and Glu: 10 mM). Control is GFP-i. For (A), (B), and (D), data are shown as mean ± SD. ns, $P \geq 0.05$; *$P \leq 0.05$; **$P \leq 0.01$; ***$P \leq 0.005$; ****$P \leq 0.0001$ (see the materials and methods for details).

previously been implicated in TORC1 signaling (*6*, *26*). For this analysis, we replenished aspartate and glutamate concentrations in *dCTNS*-overexpressing animals through dietary supplementation of anaplerotic amino acids. Treatments with combinations of alanine, aspartate, asparagine, glutamate, and proline [which replenishes glutamate in flies (*27*)] restored normal levels of aspartate and glutamate without compromising *dCTNS*-induced elevation of TCA intermediates (fig. S15, D and E). These treatments rescued the developmental delay induced by *dCTNS* overexpression in the fat body (Fig. 6B). Similarly, cosupplementation of cysteine with excess of single amino acids including alanine, aspartate, asparagine, glutamate, and proline each rescued cysteine-induced growth suppression upon fasting (Fig. 6C). In addition, treatments with a combination of amino acids restored TORC1 activity upon fasting after *dCTNS* overexpression in the fat body (Fig. 6D). Consistent with the importance of aspartate synthesis, clonal loss of *Got2* induced autophagy (*6*), inhibited TORC1 activity as indicated by decreased levels of phosphorylated 4E-BP, increased levels of the reporter Unk-GFP (*28*), and inhibited cell growth as shown by decreased nucleus size (fig. S14F). Thus, cysteine metabolism appears to regulate anaplerotic carbon flow in the TCA cycle and the level of cataplerotic products such as aspartate. We propose that lysosomal-derived cysteine converts the TCA cycle into a reservoir of carbons in the mitochondria while limiting their extraction for biosynthesis. This process may spare nutrients to allow animals to survive starvation while resetting TORC1 activity to a threshold that maintains minimal growth without compromising autophagy.

Discussion

Maintaining cellular homeostasis upon nutrient shortage is an important challenge for all animals. Decreased activity of TORC1 is necessary to limit translation, reduce growth rates, and promote autophagy. Conversely, minimal TORC1 activity is required to promote lysosomal biogenesis, thus maintaining autophagic degradation necessary for survival (*8*). Using *Drosophila* as an in vivo model, we found that TORC1 reactivation upon fasting integrates the biosynthesis of amino acids from anaplerotic inputs into the control of growth. The regulation of aspartate abundance appears to be critical during this process, possibly because it serves as a cataplerotic precursor for various macromolecules, including other amino acids and nucleotides, which in turn impinge on TORC1 activity (*29*). Cysteine recycling through the lysosome may fuel acetyl-CoA synthesis and prevent reactivation of TORC1 above a threshold that would compromise autophagy and survival during fasting. Reactivation of TORC1 during fasting was not passively controlled by the extent of amino acid remobilized from the lysosome. Instead, cysteine metabolism supported an increased incorporation of the carbons from these remobilized amino acids into the TCA cycle. We therefore propose that the remobilized amino acids may be transiently stored in the form of TCA cycle intermediates compartmentalized in the mitochondria, thereby restricting their accessibility. The regulation of TORC1 activity over a fasting period appears to be a combination of activating and suppressing cues that conciliate autophagy with anabolism. This process is self-regulated by autophagy, because autophagic protein degradation controls cystine availability through the lysosomal cystinosin transporter. Thus, in contrast to fed conditions, in which amino acid transporters at the plasma membrane maintain high cytosolic concentration of leucine and arginine that can directly be sensed by members of the TORC1 machinery (*3*), TORC1 reactivation in prolonged fasting is regulated indirectly by lysosome-mitochondrial cross-talk. Because cystinosin has also been shown to physically interact with several components of lysosomal TORC1 in mammalian cells (*14*), additional layers of regulation are conceivable during this process.

Multiple functions of cysteine impinge on cellular metabolism, including transfer RNA

thiolation, the generation of hydrogen sulfide, the regulation of hypoxia-inducible factor (HIF), and its antioxidant function through glutathione synthesis (*30*–*32*). Supplementation with cysteine or modified molecules such as *N*-acetyl-cysteine (NAC) can be used to efficiently buffer oxidative stress and perhaps alleviate symptoms of diseases that promote oxidative stress or glutathione deficiency, including cystinosis (*33*–*36*). Cysteine or NAC treatment extends the life span in flies, worms, and mice, and mice fed NAC show a sudden drop in body weight similar to that caused by dietary restriction (*18*, *37*). Our results indicate that cysteine may not only act through its antioxidant function but also by restricting the availability of particular amino acids and limiting mTOR activity, processes known to extend life span. Moreover, we show that CoA is a main fate of cysteine that affects oxidative metabolism in the mitochondria, which is the main source of reactive oxygen species (ROS). Thus, the antioxidant function of cysteine also might be coupled to its effects on the mitochondria to buffer ROS production.

In summary, we demonstrate that cysteine metabolism acts in a feedback loop involving de novo CoA synthesis, the TCA cycle, and amino acid metabolism to limit TORC1 reactivation upon prolonged fasting. This pathway may be particularly important for developing organisms that must maintain autophagy and balance growth and survival during periods of food shortage.

Materials and Methods

Fly stocks and maintenance

All flies were reared at 25°C and 60% humidity with a 12-hour on/off light cycle on standard laboratory food. N.P.'s standard laboratory food: 12.7 g/liter deactivated yeast, 7.3 g/liter soy flour, 53.5 g/liter cornmeal, 0.4% agar, 4.2 g/liter malt, 5.6% corn syrup, 0.3% propionic acid, and 1% Tegosept/ethanol. M.S.'s standard laboratory food: 18 g/liter deactivated yeast, 10 g/liter soy flour, 80 g/liter cornmeal, 1% agar, 40 g/liter malt, 5% corn syrup, 0.3% propionic acid, and 0.2% 4-hydroxybenzoic acid methyl ester (nipagin)/ethanol. Density was standardized for at least one generation before the experiments. For experiments, larvae were reared on freshly made food. *Lpp-gal4* was a gift from P. Léopold. *UAS-tsc1, UAS-tsc2* was a gift from C. Mirth (*38*). *yw,hs-Flp; mCherry–Atg8a; Act>CD2>GAL4, UAS–nlsGFP/TM6B* was a gift from E. Baehrecke. *hsFlp; act>CD2>Gal4, UAS nlsGFP* is a stock from N.P.'s laboratory (*39*). *yw, hsFlp, Tub-Gal4>UAS-nlsGFP/FM6;;neoFRT82B, TubGal80/TM6,Tb,Hu* was a gift from A. Bardin. *nprl2*^{1} and *mio*^{2} were a gift from M. Lilly. *hsFlp; R4-Gal4, UAS-mCherry-Atg8a; FRT82B UAS-GFP/TM6b* was a gift from G. Juhász. The following stocks were obtained from the Bloomington Drosophila Stock Center (BDSC) at Indiana University: *UAS-w*^{RNAi} (HMS00045), *UAS-w*^{RNAi} (HMS00017), *UAS-GFP*^{RNAi} (#9330) *attp40* (#36304), *attp2* (#36303), *UAS-mCherry-nls* (#38425), *UAS-Atg1*^{RNAi} (HMS02750), *UAS-Atg18a*^{RNAi} (JF02898), *UAS-TSC2*^{RNAi} (HM04083), *w*^{1118}, *UAS-dCTNS*^{RNAi} (HMS00213), *UAS-Got2*^{RNAi} (HMJ21924), *UAS-CPT1/whd*^{RNAi} (HMS00033), *UAS-Cbs*^{RNAi} (GL01309), *UAS-pdp*^{RNAi} (HMS018888), and *UAS-pcb*^{RNAi} (HMC04104). When comparing the effects of RNA interference (RNAi) knockdown or protein overexpression through induction of UAS-dsRNA or UAS-cDNA expression, *UAS-w*^{RNAi} (HMS00045), *UAS-w*^{RNAi} (HMS00017), *attp2* (#36303), and *attp40* (#36304) were used as controls for the TRIP collection (https://www.flyrnai.org/TRiP-HOME.html), and UAS-GFP RNAi for *dCTNS* overexpression. *dCTNS* knockout flies were generated with CRISPR/Cas9 technology according to (*40*). Two single guide RNAs (sgRNAs) using oligos (one after the ATG start codon in exon 3: GGTGATGTCATGGGAATCGA, and the other before the translation of the first transmembrane domain in exon 4: GGGCAGTACTCGAAATCAGT) were produced by polymerase chain reaction (PCR) and in vitro transcribed into RNA using the MEGAscript T7 Transcription Kit (Thermo Fisher Scientific). RNA was injected into *act-Cas9* flies (from F. Port and S. Bullock). F_0 flies were crossed to w;; TM3,Sb/TM6,Tb balancer flies and F_1 progenies were screened through PCR using oligos flanking the targeted genome region. Any indel difference >3 bp was visualized in 4% agarose gel in heterozygot F_1 progeny. To generate *dCTNS-mKate2* fusion allele, an *mKate2* open reading frame was inserted at the C terminus of *dCTNS* using a CRISPR/Cas9 endogenous tagging strategy with vectors kindly provided by Y. Bellaiche (Curie Institut, Paris). In brief, two 1-kb-long homology arms (HR1 and HR2) of the *dCTNS* gene flanking the sgRNA-guided Cas9 cutting site were cloned into a vector flanking the ATG/STOP-less *mKate2* allele (HR1-linker-mKate2-loxP-mini-white-loxP-linker-HR2). In addition, two vectors for the expression of sgRNA (sgRNA-1: CCACCGTGACCGATGTTCAAAAT, sgRNA-2: CCGAGCGAAGTGACGACTGAGAA) targeting the C-terminal coding region of *dCTNS* were generated. All three vectors were injected into *vas-Cas9* flies (BDSC, #55821) embryos by Bestgene. Progenies were screened for the red eyes (selection marker mini-*white*) and crossed to Cre-expressing flies to remove the mini-*white* by *loxP*/Cre excision. For overexpression of *dCTNS*, *dCTNS* cDNA was cloned into the Gateway destination vector pUASg-HA.attB (GeneBank: KC896837) according to (*41*). The plasmid was injected by Bestgene into embryos (BDSC, #24482) for ϕ31-mediated recombination at a *attP* insertion site on the second chromosome.

Fly food and starvation protocols

Heavy isotope tracers were from Cambridge Isotope Laboratories. All other amino acids and compounds used were from Sigma-Aldrich. In N.P.'s laboratory, compounds in solution were added to the following food mixture: 60 g/liter sucrose, deactivated yeast as a source of total protein (2 g/liter for low-protein diet, 4 g/liter for mild low-protein diet, 20 g/liter for fed fly food), 80 g/liter cornmeal, 0.35% agar, 0.3% propionic acid, and 1% Tegosept (100 g/liter in ethanol). Glucose tracing was done without sucrose and alanine tracing without yeast. In M.S.'s laboratory, fasting food had to be adapted to 6 g/liter of deactivated yeast to match control fast (2 g/liter) developmental rates observed in N.P.'s laboratory. For control food in the M.S. laboratory, the standard laboratory food was used (see protocol above). In fig. S4 specifically, 100% amino acid was 17 g/liter deactivated yeast. For fasting experiments, larvae were placed on paper wipes soaked in phosphate-buffered saline (PBS) in a petri dish.

Generation of clones

For autophagy experiments, clones were generated by crossing *yw, hs-flp; mCherry–Atg8a; Act>CD2>GAL4, UAS–nlsGFP/TM6B* with the indicted UAS lines. Progeny of the relevant genotype was reared at 25°C, and spontaneous clones were generated in the fat body because of the leakiness of the heat-shock flipase (*hs-flp*). For *dCTNS*$^{-/-}$ clones, autophagy was analyzed by crossing *w;;neoFRT82B, dCTNS*$^{-/-}$ to *hs-flp; R4-Gal4, UAS-mCherry-Atg8a; FRT82B UAS-GFP/TM6b*. For P-4EBP1 experiments, clones were either generated by crossing *hs-flp; act>CD2>Gal4, UAS nlsGFP* with the indicted UAS lines or, for *dCTNS*$^{-/-}$ clones, by crossing *w;;neoFRT82B, dCTNS*$^{-/-}$ to *yw, hs-flp, tub-Gal4>UAS-nlsGFP/FM6;;neoFRT82B, tubGal80/TM6,Tb,Hu*. F_1 embryos collected overnight were heat shocked for 2 hours at 37°C the following morning.

Amino acid screen

Larvae were fed a diet with reduced yeast extract and proteins (50% of normal diet), individual amino acids were systematically added to the food, and the time to pupariation was monitored as a proxy for growth rate. The following mixture was diluted 1:1 with amino acid solutions in water: 10 g/liter agar, 120 g/liter sucrose, 17 g/liter deactivated yeast extract, 80 g/liter cornmeal, 6 ml/liter propionic acid, and 20 ml/liter Tegosept. The amount of amino acids added to the food was determined based on those used in tissue culture growth supplements (see table S1) (*42*–*44*).

Food intake

Larvae were synchronized in L1 and reared on the indicated food types until the mid-second

instar stage. They were then transferred on the same food type supplemented with 0.5% weight/volume erioglaucine disodium salt (Sigma-Aldrich) for 2 hours. Samples were homogenized in 200 µl of PBS, and absorbance of the dye in the supernatant was measured at 625 nm. Results were normalized to protein content.

Developmental timing

Three-day-old crosses were used for 3- to 4-hour periods of egg collection on standard laboratory food. Newly hatched L1 larvae were collected 24 hours later for synchronized growth using the indicated diets at a density of 30 animals per vial. The time to develop was monitored by counting the number of animals that underwent pupariation every 2 hours in fed conditions or once or twice a day in starved conditions. The time at which half the animals had undergone pupariation was recorded.

Adult survival experiments

To generate age-synchronized adult flies, larvae were raised on laboratory food at low density, transferred to fresh food upon emerging as adults, and mated for 48 hours. Animals were anesthetized with low levels of CO_2, and males were sorted at a density of 10 per vial. Each condition contained eight to 10 vials. Each experiment was repeated at least three times, and the average values of each experiment were used for statistical analysis. Flies were transferred to fresh food vials three times per week, at which point deaths were scored. After 10 days, deaths were scored every day. Chemically defined (holidic) fasting medium was prepared following the protocol described in (*43*), which contains all physiologically relevant ions (including biometals) but lacks energy sources such as sugar, proteins, amino acids, lipids, and lipid-related metabolites, as well as nucleic acids and vitamins.

Growth curves and pupal weight

Synchronized, newly-hatched L1 larvae were immediately weighed or placed on the indicated food at a density of 30 to 50 animals per vial. Pools of 20 to 80 animals were weighed every 24 hours using an analytical scale (Mettler Toledo), and the weight was reported ± SEM. For pupal weight, 2-day-old pupae from vials at a density of 30 animals were weighed in batches of five to 10 pupae. The weights of different batches of larvae from the same vials were averaged and counted as $N = 1$.

Metabolite profiling

For whole-body metabolic profiling, 25 to 38 mid-second-instar or eight to 15 mid-third-instar larvae per sample were collected, snap-frozen in liquid nitrogen, and stored at −80°C in extraction buffer (four to six biological replicates/experiment). For fat body metabolic profiling, fat bodies from 35 to 40 larvae 96 hours after egg laying (AEL) were dissected in 20 µl of PBS, diluted in 300 µl of cold extraction buffer, and snap frozen. Tissues were homogenized in extraction buffer using 1 mm zirconium beads (Next Advance, ZROB10) in a Bullet Blender tissue homogenizer (model BBX24, Next Advance). Metabolites were extracted using 80% (v/v) aqueous methanol (two sequential extractions with 300 to 600 µl), and metabolites were pelleted by vacuum centrifugation. Pellets were resuspended in 20 µl of high-performance liquid chromatography (HPLC)–grade water, and metabolomics data were acquired using targeted liquid chromatography tandem mass spectrometry (LC-MS/MS). A 5500 QTRAP hybrid triple quadrupole mass spectrometer (AB/SCIEX) coupled to a Prominence UFLC HPLC system (Shimadzu) was used for steady-state analyses of the samples. Selected reaction monitoring (SRM) of 287 polar metabolites using positive/negative switching with hydrophilic interaction LC (HILIC) was performed. Peak areas from the total ion current for each metabolite SRM Q1/Q3 transition were integrated using MultiQuant version 2.1 software (AB/SCIEX). The resulting raw data from the MultiQuant software were normalized by sample weight for the whole animal. Fat body samples were normalized by the mean protein content measured from duplicate dissection for each condition. Data were analyzed using Prism informatic software. Alternatively, collected larvae were rinsed with water, 70% ethanol, and PBS to remove food and bacteria; snap-frozen in liquid nitrogen; and stored at −80°C until extraction in 50% methanol, 30% acetonitrile, and 20% water. The volume of extraction solution added was adjusted to larvae mass (40 mg/ml), samples were vortexed for 5 min at 4°C and then centrifuged at 16,000*g* for 15 min at 4°C. Supernatants were collected and analyzed by LC-MS using a QExactive Plus Orbitrap mass spectrometer equipped with an Ion Max source and a HESI II probe and coupled to a Dionex UltiMate 3000 UPLC system (Thermo Fisher Scientific, USA). An SeQuant ZIC-pHilic column (Millipore) was used for liquid chromatography separation (*45*). The aqueous mobile-phase solvent was 20 mM ammonium carbonate plus 0.1% ammonium hydroxide solution, and the organic mobile phase was acetonitrile. The metabolites were separated over a linear gradient from 80% organic to 80% aqueous for 15 min and detected across a mass range of 75 to 1000 m/z at a resolution of 35,000 (at 200 m/z) with electrospray ionization and polarity switching mode. Lock masses were used to ensure mass accuracy <5 ppm. The peak areas of different metabolites were determined using TraceFinder software (Thermo Fisher Scientific) using the exact mass of the singly charged ion and known retention time on the HPLC column. In total, each metabolic profiling experiment was performed at least two times with three to seven biological replicates per genotype.

TCA cycle isotopomer method from U-^{13}C-cysteine, $^{13}C_3$-$^{15}N_1$-cysteine, U-^{13}C-glucose, and U-^{13}C-alanine

Fed and starved mid-third-instar animals were supplemented with the indicated concentrations of U-^{13}C-cysteine, $^{13}C_3$-$^{15}N_1$-cysteine, U-^{13}C-glucose, U-^{13}C-alanine, or vehicle in the food for the indicated times. For tracing experiments on the low-protein diet (starved), animals were prestarved for 1 hour on PBS before being transferred to the relevant tracer and food. Samples were collected (at least five biological replicates for labeled conditions and at least four biological replicates for the unlabeled condition), and intracellular metabolites were extracted using 80% (v/v) aqueous methanol. Q1/Q3 SRM transitions for incorporation of ^{13}C-labeled metabolites were established for polar metabolite isotopomers, and data were acquired by LC-MS/MS. Peak areas were generated using MultiQuant version 2.1 software. Peak areas from unlabeled conditions were used for background determination in each experiment. In Fig. 5E and figs. S2A, S10, A and B, and S14, data for both labeled and unlabeled conditions were corrected for natural isotope abundance before normalization using the R package IsoCorrectoR GUI 1.9.0. In Fig. 4A, data for both labeled and unlabeled conditions were not corrected for natural isotope abundance. In Fig. 5E, $^{13}C_3$-alanine incorporation into the indicated isotopomer of TCA cycle intermediates was measured in control and lpp>dCTNS–overexpressing animals. Values were corrected for natural isotope abundance before normalization, and data present the fold change ^{13}C labeling in TCA cycle intermediates in dCTNS-overexpressing versus control animals.

Cysteine measurement (other than LC-MS/MS)

The 25 to 40 mid-second-instar animals were homogenized in cold PBS with 0.1% Triton X-100 (PBST) and centrifuged at 4°C. Cysteine measurement was performed in triplicate from the supernatant using the MicroMolar Cysteine Assay Kit (ProFoldin, CYS200) according to the manufacturer's instructions. Data were normalized to protein content.

Cystine measurements

Larvae were washed three times (in water, quickly in 70% ethanol, and finally in PBS), dried on tissue paper, and 10 larvae per sample were shock frozen in liquid nitrogen and stored at −80°C until lysis. Larvae were lysed in 80 µl of 5.2 mM N-ethylmaleimide, centrifuged for 10 min at 4°C, and 75 µl of supernatant was

deproteinized by the addition of 25 µl of 12% sulfosalicylic acid. Protein-free supernatants were kept frozen at −80°C until analysis and centrifuged at 1200*g* before use. Cystine quantification was performed using the AccQ-Tag Ultra kit (Waters) on a UPLC-xevoTQD system (Waters) according to the manufacturer's recommendations. Ten microliters of sample was mixed with 10 µl of a 30 µM internal standard solution (stable isotope of cystine), 70 µl of borate buffer, and 20 µl of derivative solution and incubated at 55°C for at least 10 min. Derivatized samples were diluted with 150 µl of ultrapurified water, and 5 µl of the final mixture was injected in the triple quadrupole mass spectrometer in positive mode. Transitions used for derivatized cystine quantification and the internal standard were 291.2>171.1 and 294.2>171.1, respectively. Cystine values were normalized by protein content using the Lowry's method on protein pellets.

Immunostaining

Fat body tissues from 68- to 85-hour AEL larvae were dissected in PBS with 2% formaldehyde at room temperature, fixed 20 to 30 min in 4% formaldehyde, washed twice for 10 min each in PBST 0.3 %, blocked for 30 min [PBST, 5% bovine serum albumin (BSA), 2% fetal bovine serum, and 0.02% NaN_3], incubated with primary antibodies in the blocking buffer overnight, and washed four times for 15 min each. Secondary antibodies diluted 1:200 or 1:500 in PBST were added for 1 hour and tissues were washed four times before mounting in Vectashield/4′,6-diamidino-2-phenylindole (DAPI). Rabbit anti–P-4EBP1 from Cell Signaling Technologies (CST 236B4, #2855) was diluted 1:500, rabbit anti-tRFP was from Evrogen (#AB233) and was used against mKate2 to stain *d*CTNS-mKate2. Purified polyclonal antibody against Mitf was generated in guinea pig by the company Eurogentec using the epitope CRRFNINDRIKELGTL. Samples were imaged using Zeiss LSM 780 and Leica TCS SP8 SMD confocal systems with a 40× water or oil-immersion objective, and images were processed with Fiji software.

Western blots

Tissues from 10 to 30 animals were dissected in CST lysis buffer (#9803) containing 2× protease inhibitor (Roche, #04693159001) and 3× phosphatase inhibitor (Roche, #04906845001), and homogenized using 1-mm zirconium beads (Next Advance, #ZROB10) in a Bullet Blender tissue homogenizer (model BBX24, Next Advance). Protein content was measured to normalize samples, 2× Laemmli sample buffer (Bio-Rad) was added and samples boiled for 6 min at 95°C. Lysates were resolved by electrophoresis (Mini-PROTEAN TGX Precast Gels, BioRad, PAGEr EX Gels, Lonza, or home-made SDS gels), proteins transferred onto polyvinylidene difluoride (PVDF) membranes (Immobilon P, Millipore), blocked in Tris-buffered saline with or without 0.1% Tween-20 buffer containing 3 to 6% BSA or 5% milk, and probed with P-S6K antibody (1:1000, CST 9209). After P-S6K was revealed, membranes were stripped for 5 to 30 min (Restore PLUS Buffer, Thermo Scientific, catalog #46430), washed, blocked in PBS Tween-20 buffer containing 5% dry milk, and probed with S6K antibody [1:10,000, a gift from A. Teleman (*46*)]. For normalization blots were probed with GADPH antibody (1:5000, GeneTex, #GTX100118). Data show representative results from at least two or three biological replicates (see quantification plots). Horseradish peroxidase (HRP)–conjugated secondary IgG antibodies (1:10000) were used together with the SuperSignal West Dura Extended Duration Substrate (Thermo Scientific, #34076) to detect the protein bands.

Statistics

Experiments are presented with whisker plots or show the mean ± SD or SEM. *P* values and significance were as follows: ns, $P \geq 0.05$; $^{*}P \leq 0.05$; $^{**}P \leq 0.01$; $^{***}P \leq 0.005$; and $^{****}P \leq 0.0001$. For the life span experiments shown in Fig. 3A, $N = 2$; for Fig. 3, C, E, and G, and fig. S11, $N \geq 3$. Significance was determined by a two-tailed *t* test (Mann-Whitney). $N = 1$ means average of eight to 10 vials per genotype and condition in one experiment. For the larval development (pupariation assay) results shown in Fig. 3B and fig. S7G, significance was determined by a two-tailed *t* test (Mann-Whitney); for Figs. 3, D and F; Fig. 6B; and fig. S12, C and E, one-way ANOVA followed by a Bonferroni's multiple-comparisons test was used. For cysteine measurements (Profoldin kit) shown in Fig. 2B, significance was determined by *t* test; for fig. S6A, one-way ANOVA followed by Dunnett's multiple-comparisons test was used; for fig. S7A, E, and F, two-tailed *t* test (Mann-Whitney) was used; and for figs. S8B and S9D, one-way ANOVA followed by a Bonferroni's multiple-comparisons test was used. For Western blots shown in Fig. 1A, the spline curve represents the trend over multiple experiments; for those shown in Fig. 1D and fig. S1A, significance was determined by two-way ANOVA followed by Sidak's multiple-comparisons test; for Fig. 2, D and F; Fig. 6D; and fig. S12B, one-way ANOVA followed by a Bonferroni's multiple-comparisons test was used. For the metabolomics shown in Fig. 1B (left plots), fig. S12D, fig. S13B, and fig. S15, C and D, significance was determined by one-way ANOVA followed by a Bonferroni's multiple comparisons test; in fig. S3A, two-way ANOVA followed by Sidak's multiple-comparisons test was used; for Fig. 1B (right plots); Fig. 2H; Fig. 5, B, C, and E; Fig. 6A; fig. S8, C and D; fig. S13, A and C; fig. S15, A, B, and E; and fig. S3B, two-tailed *t* test (Mann-Whitney) was used. For pupal weights shown in fig. S4C and food intakes shown in fig. S4D, significance was determined by unpaired two-tailed *t* test.

REFERENCES AND NOTES

1. D. A. Cappel *et al*., Pyruvate-carboxylase-mediated anaplerosis promotes antioxidant capacity by sustaining TCA cycle and redox metabolism in liver. *Cell Metab.* **29**, 1291–1305.e8 (2019). doi: 10.1016/j.cmet.2019.03.014; pmid: 31006591
2. L. R. Gray *et al*., Hepatic mitochondrial pyruvate carrier 1 is required for efficient regulation of gluconeogenesis and whole-body glucose homeostasis. *Cell Metab.* **22**, 669–681 (2015). doi: 10.1016/j.cmet.2015.07.027; pmid: 26344103
3. R. L. Wolfson, D. M. Sabatini, The dawn of the age of amino acid sensors for the mTORC1 pathway. *Cell Metab.* **26**, 301–309 (2017). doi: 10.1016/j.cmet.2017.07.001; pmid: 28768171
4. R. C. Scott, O. Schuldiner, T. P. Neufeld, Role and regulation of starvation-induced autophagy in the *Drosophila* fat body. *Dev. Cell* **7**, 167–178 (2004). doi: 10.1016/j.devcel.2004.07.009; pmid: 15296714
5. T.-C. Lin *et al*., Autophagy: Resetting glutamine-dependent metabolism and oxygen consumption. *Autophagy* **8**, 1477–1493 (2012). doi: 10.4161/auto.21228; pmid: 22906967
6. H. W. S. Tan, A. Y. L. Sim, Y. C. Long, Glutamine metabolism regulates autophagy-dependent mTORC1 reactivation during amino acid starvation. *Nat. Commun.* **8**, 338 (2017). doi: 10.1038/s41467-017-00369-y; pmid: 28835610
7. G. A. Wyant *et al*., NUFIP1 is a ribosome receptor for starvation-induced ribophagy. *Science* **360**, 751–758 (2018). doi: 10.1126/science.aar2663; pmid: 29700228
8. L. Yu *et al*., Termination of autophagy and reformation of lysosomes regulated by mTOR. *Nature* **465**, 942–946 (2010). doi: 10.1038/nature09076; pmid: 20526321
9. J. Colombani *et al*., A nutrient sensor mechanism controls *Drosophila* growth. *Cell* **114**, 739–749 (2003). doi: 10.1016/S0092-8674(03)00713-X; pmid: 14505573
10. C. Géminard, E. J. Rulifson, P. Léopold, Remote control of insulin secretion by fat cells in *Drosophila*. *Cell Metab.* **10**, 199–207 (2009). doi: 10.1016/j.cmet.2009.08.002; pmid: 19723496
11. W. Cai, Y. Wei, M. Jarnik, J. Reich, M. A. Lilly, The GATOR2 component Wdr24 regulates TORC1 activity and lysosome function. *PLOS Genet.* **12**, e1006036 (2016). doi: 10.1371/journal.pgen.1006036; pmid: 27166823
12. Y. Wei, M. A. Lilly, The TORC1 inhibitors Nprl2 and Nprl3 mediate an adaptive response to amino-acid starvation in *Drosophila*. *Cell Death Differ.* **21**, 1460–1468 (2014). doi: 10.1038/cdd.2014.63; pmid: 24786828
13. J. Onodera, Y. Ohsumi, Autophagy is required for maintenance of amino acid levels and protein synthesis under nitrogen starvation. *J. Biol. Chem.* **280**, 31582–31586 (2005). doi: 10.1074/jbc.M506736200; pmid: 16027116
14. Z. Andrzejewska *et al*., Cystinosin is a component of the vacuolar H+-ATPase-Ragulator-Rag complex controlling mammalian target of rapamycin complex 1 signaling. *J. Am. Soc. Nephrol.* **27**, 1678–1688 (2016). doi: 10.1681/ASN.2014090937; pmid: 26449607
15. B. P. Festa *et al*., Impaired autophagy bridges lysosomal storage disease and epithelial dysfunction in the kidney. *Nat. Commun.* **9**, 161 (2018). doi: 10.1038/s41467-017-02536-7; pmid: 29323117
16. M. Town *et al*., A novel gene encoding an integral membrane protein is mutated in nephropathic cystinosis. *Nat. Genet.* **18**, 319–324 (1998). doi: 10.1038/ng0498-319; pmid: 9537412
17. H. Kabil, O. Kabil, R. Banerjee, L. G. Harshman, S. D. Pletcher, Increased transsulfuration mediates longevity and dietary restriction in *Drosophila*. *Proc. Natl. Acad. Sci. U.S.A.* **108**, 16831–16836 (2011). doi: 10.1073/pnas.1102008108; pmid: 21930912
18. A. A. Parkhitko, P. Jouandin, S. E. Mohr, N. Perrimon, Methionine metabolism and methyltransferases in the regulation of aging and life span extension across species. *Aging Cell* **18**, e13034 (2019). doi: 10.1111/acel.13034; pmid: 31460700
19. R. O. Ball, G. Courtney-Martin, P. B. Pencharz, The in vivo sparing of methionine by cysteine in sulfur amino acid requirements in animal models and adult humans. *J. Nutr.* **136** (suppl.), 1682S–1693S (2006). doi: 10.1093/jn/136.6.1682S; pmid: 16702340

20. W. C. Rose, R. L. Wixom, The amino acid requirements of man. 13. The sparing effect of cystine on the methionine requirement. *J. Biol. Chem.* **216**, 763–773 (1955). doi: 10.1016/S0021-9258(19)81430-8
21. W. A. Gahl, F. Tietze, J. D. Butler, J. D. Schulman, Cysteamine depletes cystinotic leucocyte granular fractions of cystine by the mechanism of disulphide interchange. *Biochem. J.* **228**, 545–550 (1985). doi: 10.1042/bj2280545; pmid: 4026796
22. M. J. Holness, M. C. Sugden, Pyruvate dehydrogenase activities and rates of lipogenesis during the fed-to-starved transition in liver and brown adipose tissue of the rat. *Biochem. J.* **268**, 77–81 (1990). doi: 10.1042/bj2680077; pmid: 2188650
23. J. Lee, J. Choi, S. Scafidi, M. J. Wolfgang, Hepatic fatty acid oxidation restrains systemic catabolism during starvation. *Cell Rep.* **16**, 201–212 (2016). doi: 10.1016/j.celrep.2016.05.062; pmid: 27320917
24. T. C. Linn, F. H. Pettit, F. Hucho, L. J. Reed, Alpha-keto acid dehydrogenase complexes. XI. Comparative studies of regulatory properties of the pyruvate dehydrogenase complexes from kidney, heart, and liver mitochondria. *Proc. Natl. Acad. Sci. U.S.A.* **64**, 227–234 (1969). doi: 10.1073/pnas.64.1.227; pmid: 4312751
25. M. St. Maurice *et al*., Domain architecture of pyruvate carboxylase, a biotin-dependent multifunctional enzyme. *Science* **317**, 1076–1079 (2007). doi: 10.1126/science.1144504; pmid: 17717183
26. L. B. Sullivan *et al*., Aspartate is an endogenous metabolic limitation for tumour growth. *Nat. Cell Biol.* **20**, 782–788 (2018). doi: 10.1038/s41556-018-0125-0; pmid: 29941931
27. H. Li *et al*., *Drosophila* larvae synthesize the putative oncometabolite L-2-hydroxyglutarate during normal developmental growth. *Proc. Natl. Acad. Sci. U.S.A.* **114**, 1353–1358 (2017). doi: 10.1073/pnas.1614102114; pmid: 28115720
28. M. Tiebe *et al*., REPTOR and REPTOR-BP regulate organismal metabolism and transcription downstream of TORC1. *Dev. Cell* **33**, 272–284 (2015). doi: 10.1016/j.devcel.2015.03.013; pmid: 25920570
29. G. Hoxhaj *et al*., The mTORC1 signaling network senses changes in cellular purine nucleotide levels. *Cell Rep.* **21**, 1331–1346 (2017). doi: 10.1016/j.celrep.2017.10.029; pmid: 29091770
30. K. J. Briggs *et al*., Paracrine induction of HIF by glutamate in breast cancer: EglN1 senses cysteine. *Cell* **166**, 126–139 (2016). doi: 10.1016/j.cell.2016.05.042; pmid: 27368101
31. C. Hine *et al*., Endogenous hydrogen sulfide production is essential for dietary restriction benefits. *Cell* **160**, 132–144 (2015). doi: 10.1016/j.cell.2014.11.048; pmid: 25542313
32. S. Laxman *et al*., Sulfur amino acids regulate translational capacity and metabolic homeostasis through modulation of tRNA thiolation. *Cell* **154**, 416–429 (2013). doi: 10.1016/j.cell.2013.06.043; pmid: 23870129
33. M. AlMatar, T. Batool, E. A. Makky, Therapeutic potential of N-acetylcysteine for wound healing, acute bronchiolitis, and congenital heart defects. *Curr. Drug Metab.* **17**, 156–167 (2016). doi: 10.2174/1389200217666151210124713; pmid: 26651980
34. R. Bavarsad Shahripour, M. R. Harrigan, A. V. Alexandrov, N-acetylcysteine (NAC) in neurological disorders: Mechanisms of action and therapeutic opportunities. *Brain Behav.* **4**, 108–122 (2014). doi: 10.1002/brb3.208; pmid: 24683506
35. K. Q. de Andrade *et al*., Oxidative stress and inflammation in hepatic diseases: Therapeutic possibilities of N-acetylcysteine. *Int. J. Mol. Sci.* **16**, 30269–30308 (2015). doi: 10.3390/ijms161226225; pmid: 26694382
36. L. Pache de Faria Guimaraes *et al*., N-acetyl-cysteine is associated to renal function improvement in patients with nephropathic cystinosis. *Pediatr. Nephrol.* **29**, 1097–1102 (2014). pmid: 24326786
37. M. V. Shaposhnikov *et al*., Effects of N-acetyl-L-cysteine on life span, locomotor activity and stress-resistance of 3 *Drosophila* species with different life spans. *Aging (Albany NY)* **10**, 2428–2458 (2018). doi: 10.18632/aging.101561; pmid: 30243020
38. T. Koyama, C. K. Mirth, Growth-Blocking Peptides As Nutrition-Sensitive Signals for Insulin Secretion and Body Size Regulation. *PLOS Biol.* **14**, e1002392 (2016).
39. P. Karpowicz, Y. Zhang, J. B. Hogenesch, P. Emery, N. Perrimon, The circadian clock gates the intestinal stem cell regenerative state. *Cell Rep.* **3**, 996–1004 (2013).
40. A. R. Bassett, C. Tibbit, C. P. Ponting, J.-L. Liu, Highly efficient targeted mutagenesis of *Drosophila* with the CRISPR/Cas9 system. *Cell Rep.* **6**, 1178–1179 (2014).
41. J. Bischof *et al*., A versatile platform for creating a comprehensive UAS-ORFeome library in *Drosophila*. *Development* **140**, 2434–2442 (2013).
42. W. C. Lee, C. A. Micchelli, Development and characterization of a chemically defined food for *Drosophila*. *PLOS ONE* **8**, e67308 (2013).
43. M. D. Piper *et al*., A holidic medium for *Drosophila melanogaster*. *Nat. Methods* **11**, 100–105 (2014).
44. A. M. Troen *et al*., Life span modification by glucose and methionine in *Drosophila melanogaster* fed a chemically defined diet. *Age (Dordr.)* **29**, 29–39 (2007).
45. G. M. Mackay, L. Zheng, N. J. F. van den Broek, E. Gottlieb, "Analysis of cell metabolism using LC-MS and isotope tracers," in *Metabolic Analysis Using Stable Isotopes*, C. M. Metallo, Ed. (Academic, 2015), *Methods in Enzymology* series, vol. 561, pp. 171–196.
46. K. Hahn *et al*., PP2A regulatory subunit PP2A-B' counteracts S6K phosphorylation. *Cell Metab.* **11**, 438–444 (2010).

ACKNOWLEDGMENTS

We thank E. Baehrecke, C. Mirth, P. Léopold, A. Teleman, F. Wirtz-Peitz, Y. Bellaïche, I. Gaugue, S. Sanquer, A.-C. Boschat, M. A. Lilly, and the TRIP (https://www.flyrnai.org/TRiP-HOME.html), BDSC, and VDRC stock centers for providing stocks and reagents; the Microscopy Resources on the North Quad (MicRoN) core at Harvard Medical School; A. Comjean for help with the R package IsoCorrectoR GUI 1.9.0; and C. Antignac, L. C. Cantley, B. Gasnier, J. D. Rabinowitz, and D. M. Sabatini for comments on the manuscript. **Funding:** This work was supported by the Cystinosis Research Foundation (P.J., Z.M., M.S., and N.P.), the LAM Foundation (fellowship award LAM00105E01-15 to A.P.), the National Institutes of Health (grant 5P01CA120964-04 to J.M.A. and N.P. and grant R01AR057352 to N.P), the National Institutes of Health and the National Cancer Institute (grant R00-CA194314 to C.C.D.), the V Foundation for Cancer Research (V Scholar Grant 2019 V2019-009 to C.C.D), the European Research Council (ERC) under the European Horizon 2020 research and innovation program (grant 865408, to M.S.), the Deutsche Forschungsgemeinschaft Heisenberg-Programm (grant DFG SI1303/5-1, to M.S.), the Fondation Bettencourt-Schueller (Liliane Bettencourt Chair of Developmental Biology, to M.S.), and state funding by the Agence Nationale de la Recherche (ANR) under the "Investissements d'avenir" program (grant ANR-10-IAHU-01 to M.S.) and NEPHROFLY (grant ANR-14-ACHN-0013 to M.S.). N.P. is an investigator of the Howard Hughes Medical Institute. **Author contributions:** P.J., Z.M., C.C.D., M.S., and N.P. designed the experiments. P.J., Z.M., Y.-H.S., A.P., M.D., J.A., and I.N. performed the experiments. P.J., Z.M., M.S., and N.P. participated in interpretation of data. P.J. wrote the manuscript with inputs from Z.M., C.C.D., M.S., and N.P. **Competing interests:** The authors declare no competing interests. **Data and materials availability:** All data are available in the main text or the supplementary materials.

SUPPLEMENTARY MATERIALS

science.org/doi/10.1126/science.abc4203
Supplementary Text S1 and S2
Figs. S1 to S15
Tables S1
References (*47*–*50*)
MDAR Reproducibility Checklist

View/request a protocol for this paper from *Bio-protocol*.

23 April 2020; accepted 12 January 2022
10.1126/science.abc4203

Science

Lysosomal cystine mobilization shapes the response of TORC1 and tissue growth to fasting

Patrick JouandinZvonimir MareljaYung-Hsin ShihAndrey A. ParkhitkoMiriam DambowskyJohn M. AsaraIvan NemazanyyChristian C. DibbleMatias SimonsNorbert Perrimon

Science, 375 (6582), eabc4203. • DOI: 10.1126/science.abc4203

Cystine as lysosomal fasting signal

Communication between the lysosome and mitochondria appears to help maintain control of metabolism in fruit flies deprived of food for prolonged periods. When food is limited, the target of rapamycin complex 1 (TORC1) protein kinase complex is inhibited, which promotes catabolism and autophagy to provide nutrients. Newly supplied amino acids could reactivate TORC1, but Jouandin *et al*. implicated cystine released from lysosomes in allowing continued catabolism during prolonged fasting. Cystine, when reduced to two molecules of cysteine, may promote the transient storage of remobilized amino acids in the form of tricarboxylic acid cycle intermediates in the mitochondria, thus limiting TORC1 reactivation during a prolonged fast. —LBR